

Achilles Tendons from T-Lymphocyte Deficient Mice Exhibit Improved Healing

Connie S Chamberlain^{1*}, Amy Ticknor¹, Linzie A Wildenauer¹, Geoffrey S Baer¹, Andrea M Spiker¹, Matthew A Halanski¹, Ugeun Choi^{1,2}, Ray Vanderby^{1,2} and Anna EB Clements²

¹Department of Orthopedics and Rehabilitation, University of Wisconsin-Madison, Madison, USA

²Department of Biomedical Engineering, University of Wisconsin-Madison, Madison, USA

*Corresponding author: Chamberlain CS, Department of Orthopedics and Rehabilitation, University of Wisconsin-Madison, Madison, WI 53705, USA, Tel: + (608) 263-7887; Fax: (608)-262-2989; E-mail: Chamberlain@ortho.wisc.edu

Received date: June 22, 2019; Accepted date: July 6, 2019; Published date: July 13, 2019

Copyright: © 2019 Chamberlain CS, et al. This is an open-access article distributed under the terms of the Creative Commons Attribution License, which permits unrestricted use, distribution, and reproduction in any medium, provided the original author and source are credited.

Abstract

Purpose/Aim of Study: Tendon healing involves a complex, coordinated series of events that, despite new therapies to improve healing, results in scar. The “nude” T-lymphocyte deficient model is a genetic strain exhibiting a loss of function in the *Foxn1* gene. Nude mice cannot generate mature T-lymphocytes, are unable to mount many types of adaptive immune responses, and were initially used as skin injury healing models. Their ability to heal external ear injuries, similar to the regenerating MRL mouse model, has since been described. We therefore hypothesized the *Foxn1*^{-/-} nude T-lymphocyte deficient mouse strain would improve tendon healing.

Materials and Methods: *Foxn1*^{-/-} T-lymphocyte deficient mice were subjected to Achilles tendon injury. Tissue was collected 7 and 14 days after injury and used to examine mechanical, cellular, compositional, and organizational effects on healing.

Results: T-lymphocyte deficient healing tendons exhibited improved stiffness, smaller wound size, decreased M1/M2 macrophage ratio, increased type III collagen, and an earlier but transient up regulation of endothelial cells compared to genetic controls.

Conclusion: The mechanisms involved in improved tendon healing of the T-lymphocyte deficient mouse may include a number of factors such as the ablation of *Foxn1*. However, the deficiency in T-lymphocytes and change in M1/M2 ratio may also impact healing by serving a regulating, protective and/or accelerating role. Overall, the clinical implication of modulating the immune cells to stimulate healing are profound and suggests the possibility to manipulate certain subsets of T-lymphocytes and/or macrophages at specific healing stages to significantly enhance musculoskeletal healing.

Keywords: Tendon; Injury; T-lymphocytes; Macrophages; *Foxn1*

Introduction

Tendon healing follows a complex sequence of coordinated events that ultimately produces a mechanically inferior tissue more scar-like than native tendon. Despite new surgical techniques and therapies to improve healing and/or minimize fibrosis, the quality and speed of repair remain problematic with prolonged healing times and extended periods of immobilization [1-4]. The repaired neo-tendinous tissue eventually results in a functionally/mechanically inferior tissue compared to its original state. An improved healing scenario would include a reduction in wound size, an increase in the type I/III collagen ratio and collagen organization, and similar structural and material properties as the original tissue.

One strategy to reduce scar formation is to modulate the endogenous immune cells localizing to the wound such that they become “effectors” of a more regenerative response. During normal healing, the innate immune system rapidly activates resident immune cells, which signal in circulating neutrophils and monocytes. Neutrophils are the first inflammatory cells to arrive at the injury and immediately begin to clear necrosed cells and debris. Inflammatory

M1 macrophages and to a lesser extent the anti-inflammatory M2 macrophages infiltrate the wound and surrounding tissue, release cytokines, and further phagocytose cell debris. Thereafter, T-lymphocytes arrive, albeit in much lower numbers. This cellular profile during early healing ultimately results in a scar-like replacement tissue. Our goal has been to mediate a more anti-inflammatory wound environment, which favors improved tendon healing. A number of studies, including our tendon and ligament experiments, have demonstrated therapeutic methods to improve healing by accelerating the transition of macrophages from an inflammatory M1 phenotype to an anti-inflammatory M2 phenotype [5,6]. However, macrophages also influence the inflammatory behavior of T-lymphocytes by serving as a bridge between innate and adaptive immunity, acting as Antigen Presenting Cells (APC) to induce T-lymphocyte maturation, and polarizing CD4⁺ T helper lymphocytes to a Th1 or Th2 phenotype. As an example, the polarized inflammatory Th1 lymphocytes produce interferon γ (IFN- γ), which stimulate M1 macrophages to kill intracellular pathogens as well as CD8⁺ cytotoxic T cells. Anti-inflammatory Th2 lymphocytes produce interleukin-4 (IL-4) to polarize macrophages to an anti-inflammatory M2 a phenotype, altogether supporting the concept that alteration of the macrophage

and/or T-lymphocyte populations provides a mechanism that may reduce inflammation and stimulate healing.

The role of T-lymphocytes is well accepted in adaptive immune pathologies, but their contribution to normal, aseptic tendon/ligament healing is considered minimal, partly due to their low abundance within the healing tissue. Although few T-lymphocytes are generally found within the uninjured and normal non-immunogenic, healing tendon/ligament, their presence has been associated with tendon and ligament injury and fibrosis [7-11]. Canines with cranial cruciate ligament rupture, a degenerative condition with unknown mechanism, have significantly increased T-lymphocytes in their synovium [12,13]. As synovitis increased in severity, so did the number of T-lymphocytes. Similarly, within rat flexor tendon and medial collateral ligament injury models, the number of T-lymphocytes increased within the injured epiligament/epitenon [10,14,15]. Additional *in vitro* co-culture studies indicated that T-lymphocytes contributed to epitenon-induced adhesion and Extracellular Matrix (ECM) formation [14]. Within other rodent injury models, significant changes in T-lymphocytes were also noted after ligaments/tendons were treated with Mesenchymal Stem/Stromal Cells (MSCs) and anti-inflammatory cytokines, suggesting that T-lymphocytes may play a greater role in tendon healing and scar formation than previously recognized [5,7,16].

The T-lymphocyte deficient model (aka “nude”) is a genetic strain exhibiting a loss of function in the *Foxn1* gene to result in a hairless phenotype in mice, rats, and humans [17]. These nude mice, originally used as healing models for skin injuries, cannot generate mature T-lymphocytes and consequently are unable to mount many types of adaptive immune responses [18]. One difference noted between nude and wild type skin healing models was in the rate of healing. Compared to its genetic control, the nude mouse had accelerated wound closure, earlier presence of granulation tissue, and an absence of disorganized collagen bundles [19]. In a nude mouse spinal cord injury model, fibrosis and post-contusion behavioural recovery patterns were also improved [20]. Based on these reported improvements to wound healing, we hypothesized the *Foxn1*^{-/-} nude T-lymphocyte deficient mouse strain would improve early tendon healing over their controls. Our results indicated that Achilles tendons from T-lymphocyte deficient mice exhibited improved mechanics, smaller wound size, decreased M1/M2 macrophage, and an earlier but transient upregulation of endothelial cells compared to its genetic control. These results also suggest that wound healing experiments using this accepted mouse strain for xenogenic experimentation should be carefully interpreted.

Materials and Methods

Achilles tendon healing model

All procedures were approved by the University of Wisconsin-Madison Institutional Animal Care and Use Committee. All surgeries were performed using isoflurane for anesthesia. Skeletally mature (9-10 weeks old) male *Foxn1*^{nu-/-} (“T-Cell Def.”; Jackson laboratory, Bar Harbor, ME; JAX stock # 002019) and *Foxn1*^{+/-} (“CX”; Jackson laboratory, Bar Harbor, ME) mice were used as an animal model to study the T-lymphocyte effect on Achilles tendon healing after surgical transection. Heterozygous *Foxn1*^{+/-} mice exhibit no altered phenotype and served as the injured control. A surgically transected rather than torn tendon was used to create a uniform defect for healing comparisons. A total of 27 mice were subjected to unilateral Achilles tendon transection. For this procedure, a skin incision was made,

fascia incised and the tendon exposed on the right hind limb. The Superficial Digital Flexor (SDF) tendon was separated from the Achilles tendon and removed. The Achilles tendon was then completely transected at the mid-point (halfway between the calcaneal insertion and the musculotendinous junction) and tendon ends were sutured together using 5-0 Vicryl suture. The left Achilles tendon remained intact and served as a contralateral control. Following transection and repair of Achilles tendon the tarsal/hock joint was immobilized using a wire cerclage. Animals were removed from trial if suture repair (slipped knot, broken suture, large gap over 0.55 mm) or tarsal immobilization failed, or if mouse exhibited severe symptoms of *C. bovis* infection. A total of 5 mice were removed from trial due to failed tarsal immobilization (n=4) and *C. bovis* infection (n=1). This resulted in a total of 27 mice included in the study. Tendons were collected at days 7 and 14 post-injury and used for mechanical testing (n=5 mice/strain, day 14 only), Immunohistochemistry (IHC) or histology (n=3 mice/strain/day). Days 7 and 14 were chosen to study treatment effects on early tendon healing with specific focus on endogenous macrophages, which are peaking in number at 7 days post-injury. Day 14 was chosen to measure angiogenesis as well as early Extracellular Matrix (ECM) formation. Day 14 was also chosen as a time that the tendon would be healed sufficiently to assay early tissue function via mechanical testing. Tendons used for IHC were carefully dissected and immediately embedded longitudinal/frontal, in optimal cutting temperature medium for flash freezing. Animals used for mechanical testing were sacrificed and limbs were stored into at -70 °C until processed. Mechanical testing was not performed on day 7 specimens because tendons were too structurally compromised for meaningful data with our experimental methods.

Immunohistochemistry/histology

IHC and histology were performed to identify cellular and ECM changes within the healing tendon on day 7 and 14 injured Achilles tendons. Longitudinal cryosections (approximately 6 sections/slide) were cut at a 5 µm thickness, mounted on Colorfrost Plus microscope slides and maintained at -70 °C. IHC was performed on frozen sections. Cryosections were fixed in acetone, exposed to 3% hydrogen peroxide to eliminate endogenous peroxidase activity, blocked with Rodent Block M (RBM961L, Biocare Medical, Pacheco, CA) and incubated with rabbit or rat primary antibodies. Primary rat monoclonal antibodies (all 1:100 from BioRad, Hercules, CA) specific to mouse F4/80 (MCA497GA), CD206 (MCA2235GA), CD31 (MCA2388GA) were used to detect total macrophages, M2 macrophages, and endothelial cells, respectively. Rabbit polyclonal antibodies were used for type I collagen (1:800, ab34710, Abcam-Serotec, Raleigh, NC) and type III collagen (1:150, ab7778, Abcam-Serotec). Lastly, rabbit monoclonal CCR7 was used to identify M1 macrophages (1:1200, ab32527 Abcam-Serotec). After primary antibody incubation, samples were exposed to rabbit (RMR622H, Biocare Medical, Pacheco, CA) or rat (BRR4016H, Biocare Medical, Pacheco, CA) Horseradish Peroxidase (HRP) Polymer. The bound antibody complex was visualized using diaminobenzidine (DAB, NB314SBD, Innovex Biosciences). Stained sections were dehydrated, cleared, cover-slipped and viewed using light microscopy. After IHC staining, micrographs were collected using a camera-assisted microscope (Nikon Eclipse microscope, model E6000 with an Olympus camera, model DP79). On average, 4.7 (± 0.20) were captured and counted per animal. Images captured for measurement of total macrophages, M1 and M2 macrophages, endothelial cells, type I collagen and type III collagen were quantified *via* Image J (National

Institutes of Health, Bethesda, MD). Measurements were collected 1) within the granulation tissue and 2) within the entire section. More specifically, total protein within the tendon was collected by first outlining the entire tendon using the polygon selection tool in Image J. Protein within the granulation tissue was also measured by outlining, measuring, and enumerating protein specifically within the granulation tissue. Protein was quantified as density/mm². Tendon cryosections were also Hematoxylin and Eosin (H&E) stained to observe histological morphology of the healing tendon.

Fractal analysis

Tissue organization was quantified by fractal dimension [21-23]. Fractal analysis assigns an objective number (fractal dimension) to an image, which quantifies its level of organization (or disorganization). It is a useful method to quantify collagen matrix organization, providing a metric to compare fibrotic scar formation between treatment groups [23]. Tissue sections were H&E stained and images were captured. H&E images were cropped 4.5×4.5 inches to include the transected region. Images were converted from gray-scale to binary images using a threshold value that was automatically determined using the automatic gray-thresh command in MATLAB (Mathworks, Natick, MA). Fractal analysis of each binary image was performed using a MATLAB routine, which calculated the fractal dimension using a Minkowski-Bouligand dimension (i.e. box counting dimension) method [24]. Fractal values range from 0-1 with a smaller fractal dimension indicating a more linearly organized tissue.

Mechanical testing

In order to determine the mechanical properties of the healing tendons, day 14 injured tendons were tested. Achilles tendons were dissected and surrounding tissue excised with care to keep the calcaneal insertion site intact. Sutures were not removed from the injured Achilles tendons 1) based on our preliminary tests indicating that sutures carried no significant load and 2) to avoid disruption of the injured region. Tendons remained hydrated using Phosphate Buffered Saline (PBS). Tendon length, width, and thickness were repeatedly measured using digital calipers and the cross-sectional area (assumed to be an ellipse) was estimated. Tendons were tested in a custom-designed load frame, which gripped and loaded the tendons along their longitudinal axis. The calcaneus was trimmed and press-fit into a custom bone grip. The soft tissue end of the specimens was fixed with adhesive (cyanoacrylate) between two plates forming the soft-tissue grip. Dimensional measurements for the tendons were recorded at pre-load. Mechanical testing was performed at room temperature. A low preload of 0.1 N was applied in order to obtain a uniform zero point 14 prior to preconditioning (20 cycles at 0.5 Hz) to 0.5%. Pull-to-failure testing was performed on tendons at a rate of 3.33 mm/sec. Force and displacement data from the test system were recorded at 10Hz. Failure force was the highest load prior to a complete rupture of the tendon and stress was calculated by dividing the failure force by the initial cross-sectional area.

Statistical analysis

A one-way Analysis of Variance (ANOVA) was used to examine differences for the IHC data. If the overall p-value for the F-test in ANOVA was significant ($p \leq 0.05$), post-hoc comparisons were performed using the Fisher's Least Significant Difference (LSD)

method. Mechanical data were analyzed *via* Student's T-Test. Experimental data are presented as the means \pm standard error of the mean (S.E.M.). $P \leq 0.05$ was the criterion for statistical significance. Computations and figures were performed using Kaleida Graph, version 4.03 (Synergy Software, Inc., Reading, PA).

Results

IHC of cellular factors

Tendon injury significantly increased the number of macrophages with the tendon regardless of mouse genotype at both 7 and 14 days after injury (Figure 1A). However, the number of macrophages within the T-Cell Def. tendon was significantly greater 7 days after injury compared to the day 7 CX (Figures 1A, G and H). The number of macrophages was not different between genotypes 14 days after injury. Further analysis of the macrophage immunophenotypes indicated that the number of inflammatory M1 macrophages increased 14 days after injury regardless of the mouse genotype (Figures 1B, I and J). No other changes were noted. In contrast, the number of anti-inflammatory M2 macrophages was significantly higher within the uninjured T-Cell Def. Achilles tendon compared to the uninjured CX (Figures 1C, K and L). Injury to the tendon resulted in more M2 macrophages localized within granulation tissue of the day 7 T-Cell Def. tendons compared to the day 7 CX tendons (Figures 1D, M and N). By 14 days post-injury, T-Cell Def. tendons exhibited significantly higher numbers of M2 macrophages throughout the tendon compared to the CX tendons at the same time (Figures 1B, O and P). The changes in immunophenotypes resulted in a higher M1/M2 ratio in the day 14 injured CX compared to the T-Cell Def. tendons (Figure 1E). Lastly, the effects of genotype on endothelial cells during healing were examined. No differences were noted between the uninjured T-Cell Def. and CX tendons whereas day 7 injured tendons from T-Cell deficient mice had significantly more endothelial cells compared to any other groups (Figures 1F, Q and R). By day 14 of injury, endothelial cell levels of the T-Cell Def. tendons were similar to the CXs.

Collagen production and organization

To examine the effects of T-cell deficiency on ECM repair and scar formation, factors including granulation tissue size, collagen production and organization were examined *via* histology, IHC and fractal analysis, respectively. Measurements of the healing region indicated that the granulation tissue size was significantly smaller within the T-Cell Def. tendon compared to the CX, 14 days after injury (Figures 2A, G-L). IHC assays examined the effect of genotypes on types I and III collagen localization after injury. As expected, more type I collagen was localized within the uninjured tendons compared to the injured (Figure 2B). However, no genotype differences were noted across time (Figure 2B). Similarly, no differences were noted in total type III collagen (Figures 2C, M and P). However, within the granulation tissue, type III collagen levels were higher in the day 7 injured T-Cell Def. tendons compared to injured CXs (Figures 2D, O and P). Levels between genotypes were similar by day 14. Further analysis of the type I/III collagen ratio indicated no differences between the two genotypes (Figure 2E). Lastly, fractal analysis showed the uninjured tissue was more organized than injured tissue, regardless of genotype (Figure 2F). No other differences were noted.

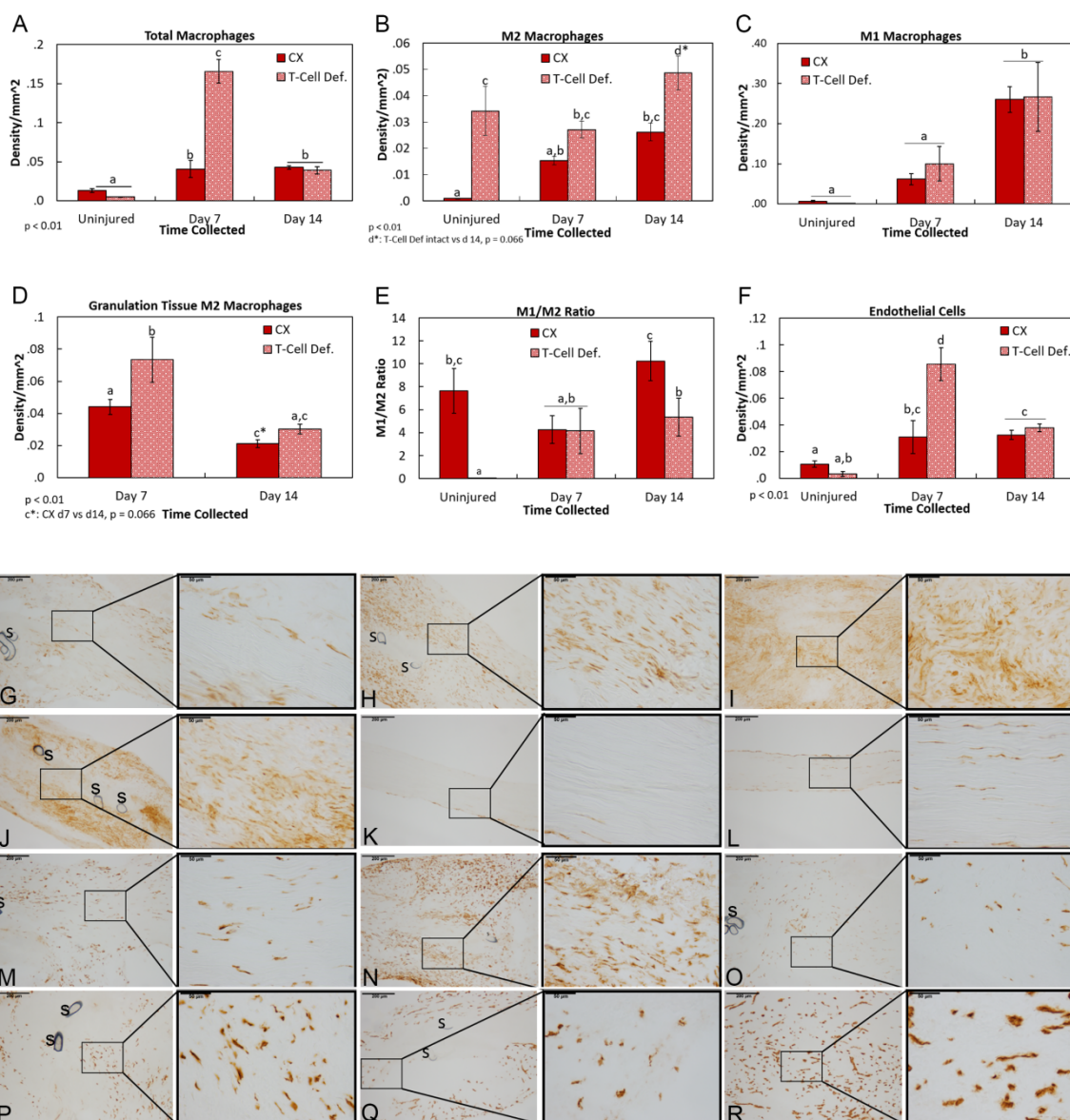


Figure 1: Immunohistochemistry analysis of cellular factors within the T-lymphocyte deficient Achilles tendon. (A) The total number of F4/80+ macrophages were significantly increased within the day 7 injured T-lymphocyte deficient (“T-Cell Def.”) Achilles tendon. By day 14, no changes were noted, (B) The M1 macrophages throughout the tendon were increased across time, regardless of phenotype, (C) The number of total M2 macrophages throughout the tendon were significantly increased within the uninjured T-Cell Def. and day 14 tendon, (D) Within the granulation tissue, M2 macrophages were significantly increased within the day 7 T-Cell Def. tendons (E) The M1/M2 ratio was significantly lower within the uninjured and day 14 injured T-Cell Def. tendons, (F) The number of endothelial cells throughout the tendon were significantly higher within the T-Cell Def. tendon 7 days after injury. By 14 days after injury, levels were similar between genotypes, (G) Representative tendon images of the: day 7 F4/80+ total macrophages within the (G) CX and (H) T-Cell Def.; day 14 M1 macrophages by the (I) CX and (J) and T-Cell Def.; M2 macrophages within uninjured (K) CX and (L) T-Cell Def.; Day 7 M2 macrophages by the (M) CX and (N) and T-Cell Def.; Day 14 M2 macrophages by the (O) CX and (P) and T-Cell Def.; and day 7 endothelial cells by the (Q) CX and (R) and T-Cell Def. samples, (G-R) Each sample includes a representative low magnification (left) and high magnification (right) image. S, indicates suture, (A-F) within each graph, p value indicates ANOVA results. a,b,c,d indicates within each graph, bars without a common superscript letter differ as a result of Fishers LSD post-hoc pairwise analysis, $p \leq 0.05$. Results are expressed as Mean \pm S.E.M. CX, *Foxn1*^{+/+}; T-Cell Def, *Foxn1*^{-/-}.

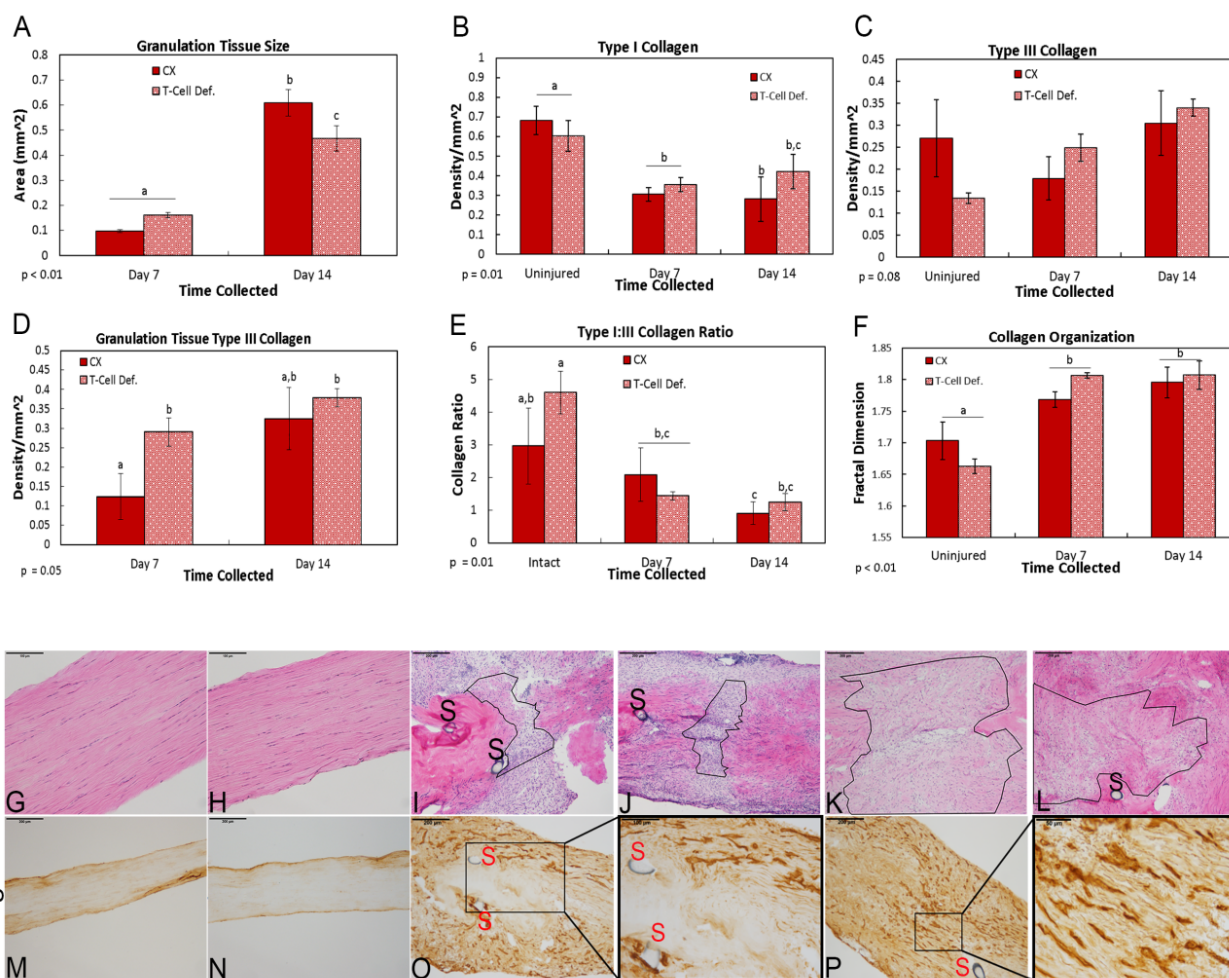


Figure 2: Changes in ECM factors within the T-lymphocyte deficient Achilles tendon. (A) The granulation tissue size was significantly smaller by the T-lymphocyte deficient (T-Cell Def.) Achilles tendon 14 days after injury compared to the injured control (CX); (B) Type I collagen levels were significantly reduced after injury, but no significance was noted between genotypes; (C) No significant changes were noted in total type III collagen (D) However, within the granulation tissue, type III collagen was significantly increased within the T-Cell Def. Achilles compared to the CX 7 days after injury (E) Type I:III collagen ratio was reduced after injury, but no other changes were noted; (F) Collagen organization was also reduced after injury. However, no changes were noted between genotypes. Representative images of (G-L) H&E staining and (M-R) type III collagen, within the (G, M) uninjured control, (H, N) uninjured T-Cell Def., (I, O) Day 7 CX, (J, P) Day 7 T-Cell Def., (K) Day 14 CX and (L) Day 14 T-Cell Def. Achilles tendons, (O-P) includes a representative low magnification (left) and high magnification (right) image. Within each graph, p value indicates ANOVA results. a,b,c indicates within each graph, bars without a common superscript letter differ as a result of Fishers LSD post-hoc pairwise analysis, $p \leq 0.05$. Results are expressed as Mean \pm S.E.M. CX, *Foxn1*^{+/+}; T-Cell Def, *Foxn1*^{-/-}; (H&E), Hematoxylin and Eosin; S: indicates suture.

Mechanical results

Tendons were first measured for length and cross sectional area. No differences were noted between CX and T-Cell Def. groups within the uninjured, day 7, or day 14 tendons ($p > 0.05$). Then, tendon tensile strength, stiffness, ultimate stress, and Young's modulus, and were measured using uni-axial tensile testing (Figure 3). No significance was noted in mechanical behaviour between the uninjured T-Cell Def. and

CX tendons. Injury to the tendons resulted in significant structural mechanical changes between groups. Specifically, within the day 14 injured tendons, structural stiffness was significantly increased ($p = 0.02$) within the T-Cell Def. tendons compared to the injured CXs (Figure 3B). No differences were found between groups for Young's modulus and ultimate stress ($p > 0.05$; Figures 3C and D).

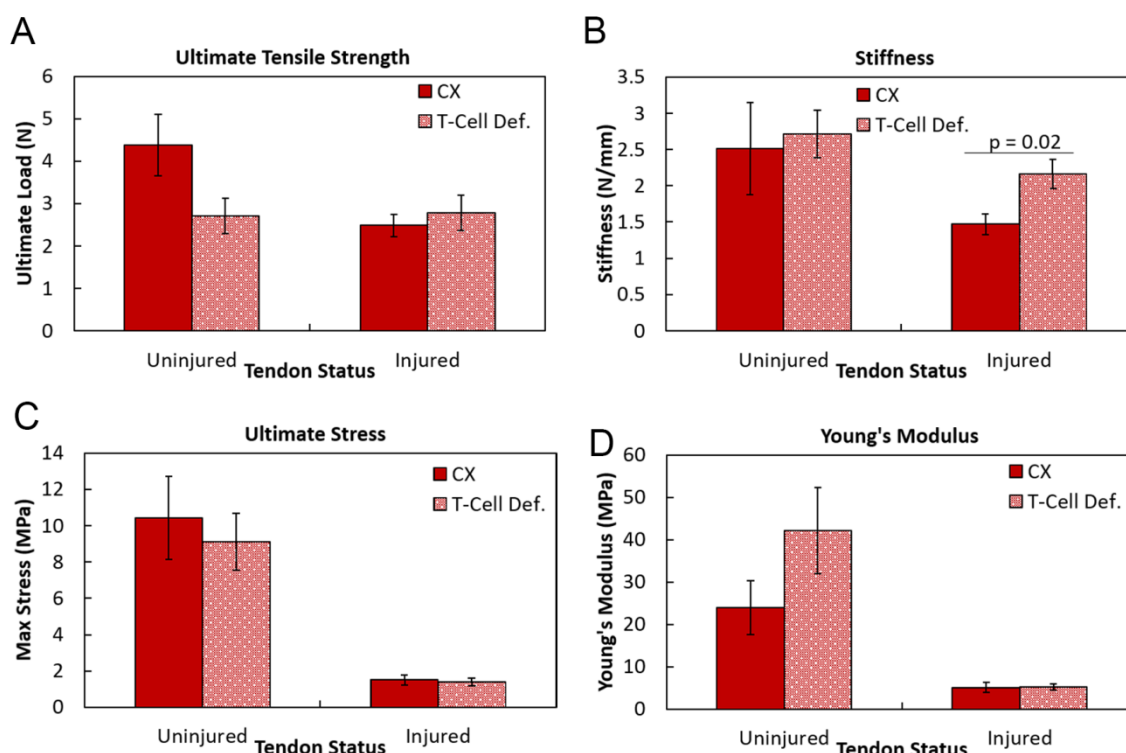


Figure 3: Mechanical testing results of the Achilles tendon by nude mice. Tendons from T-lymphocyte deficient (T-Cell Def.) mice were collected from uninjured as well day 14 injured tendons and compared to heterozygous mice (CX). (A) No significant differences were noted in the ultimate tensile strength between the CX and T-Cell Def. groups within the uninjured ($p=0.08$) and injured ($p=0.56$) tendons; (B) Stiffness was significantly increased ($p=0.02$) between the T-Cell Def. and CX animals 14 days after injury. No changes were noted in; (C) ultimate stress; and (D) Young's modulus. Within each graph, p value indicates Student's T-Test results. Significance was based on $p \leq 0.05$. Results are expressed as Mean \pm S.E.M. CX, *Foxn1*^{+/+}; T-Cell Def, *Foxn1*^{-/-}.

Discussion

In this study T-cell deficient mice were able to augment tendon healing greater than their genetic controls as indicated by improved stiffness, reduced inflammatory response, smaller wound size, and accelerated production of collagen. Unfortunately, no mammalian regenerative tendon model currently exists but improved healing has been reported in the MRL/MpJ mouse, rodent neonate, and fetal sheep [25-27]. The MRL/MpJ mouse presents varying degrees of healing in ears, cornea, heart, spinal cord, and articular cartilage [28-32]. Within the patellar tendon injury model, MRL mice improved mechanical properties but tenogenic expression patterns were not different between scar forming C57Bl/6 mouse tendons [26]. The injured Achilles tendon within the mouse neonate likewise fully recovered functional properties, but collagen matrix was not completely repaired [25]. In contrast, injury to lateral extensor tendon in fetal sheep resulted in restored matrix but similar mechanical properties as the scarring adult tendon [27]. Tendon injury to the T-cell deficient mouse model likewise does not result in regeneration but improved healing is evident.

In studies with other types of injuries, the T-cell deficient mouse has previously shown a capability for improved healing. Studies of spinal cord injuries and skin repair using the nude mouse models, both have

demonstrated significantly improved healing compared to wild type mice. In spinal cord healing, nude mice demonstrated reduced scar and improved recovery of post-contusion behavior [20]. Skin healing improvements included accelerated wound closure, earlier presence of granulation tissue, absence of disorganized collagen bundles, and augmented mechanical function [18,19,33-36]. Our tendon healing experiments agree with the skin and spinal cord injury models in that the tendon stiffness was improved.

Tendon healing changes within the nude model may involve three possible interrelated mechanisms including *Foxn1* gene ablation, T-lymphocyte modulation, and/or M2 macrophage upregulation. Consider first, the role of *Foxn1* gene ablation. The nude mouse model is generated *via* point mutation of the transcription factor *Foxn1*, a member of the forkhead/winged-helix class of transcription factors expressed in the thymus and skin epithelial cells [17]. The *Foxn1* point mutation results in athymic mice and the inability to produce mature T-lymphocytes. Scar-free healing in mammalian fetuses and nude mice has been shown to coincide with the reduction in *Foxn1* expression [37]. For example, skin healing transitions from scar-free to scar-forming in mouse fetuses at day 16 of gestation. Within the mouse skin, *Foxn1* is expressed 16-17 days post gestation and continues to increase until 3 weeks after birth. Thereafter, *Foxn1* levels decline as the mouse ages. It is possible that the mutation in *Foxn1* nude mice

provides conditions favorable to healing. However, the regenerating MRL mouse model does not exhibit genetic anomalies with the *Foxn1* gene, thus suggesting that *Foxn1* is unlikely to play a direct role in healing. To further examine the role of *Foxn1*, a study was conducted to measure *Foxn1* overexpression on cell function. Overexpression of *Foxn1* by keratinocytes stimulated early differentiation and suppressed later differentiation, indicating that *Foxn1* plays more of a role in modulating terminal cell differentiation [38]. More recently, a study comparing the genetic profile between injured skin from *Foxn1* null mice and regenerating embryonic day 14 mice was performed. Those results indicated that lack of *Foxn1* maintains tissue in an immature stage of development, which also suggested that *Foxn1* was not the main determinant in the regenerating process and instead played a regulatory role in cell differentiation [39].

A second proposed mechanism for improved healing in the nude mouse attributes to the depletion of T-lymphocytes. Numerous studies have reported improved healing after T-lymphocyte depletion. In particular, reduced levels of CD8⁺ T-lymphocytes increased wound strength and healing [34,40-42] whereas re-application of T-lymphocytes back into the skin injury of the nude mouse resulted in decreased wound breaking strength [18]. Similar to the nude mouse, the MRL mouse also exhibits abnormalities in T-lymphocyte population without a mutation in the *Foxn1* gene [43]. Although evidence points more towards the T-lymphocyte deficiency (*vs. Foxn1* gene deletion) as the mechanism affecting healing, more research is required.

The last proposed mechanism of improved healing within a T-cell deficient model involves the upregulation of the M2 macrophages. Our T-cell deficient mouse model exhibited significantly higher levels of M2 macrophages within both the intact and day 14 healing tendons. Numerous studies have indicated that the upregulation of M2 macrophages improves wound healing. Within the nude mouse model, skin incision wounds not only exhibited improved healing, but also demonstrated significantly higher levels of macrophage activity [44]. When these nude mice were subjected to thymus transplantation, the elevated macrophage levels were either totally or partially returned to values found in thymus-bearing animals [44]. Our current Achilles tendon study also indicates a significantly increased number of resident M2 macrophages within the uninjured T-cell deficient mouse tendon. The presence of these resident M2 macrophages within the intact tissue may serve a protective role and allow a faster anti-inflammatory response to injury by the T-cell deficient animals. A study in mice showed that endotoxin preconditioning to increase the M2 macrophages within the uninjured tissue served a protective role on renal tubules after injury [45]. Similar results were found with the rat hippocampus, which demonstrated a neuroprotective effect by reducing the M1/M2 ratio [46]. Within our Achilles tendon injury model, a higher number of M2 macrophages within the intact tissue were also associated with an increase in type III collagen, a higher number of endothelial cells, and stiffness closer to intact tissue within the injured tissue. Interestingly, M2 macrophages remained higher within the day 14 T-cell deficient tendons when compared to the injured controls. This continued upregulation of M2 macrophages in the T-cell deficient mouse resembles the macrophage patterning of the amputated salamander limb, a well-accepted model of regeneration. Amputation of a regenerating salamander limb results in the early and extended upregulation of M2 macrophages and anti-inflammatory cytokines [47]. In contrast, the onset of a scar-forming mammalian injury is typically characterized by an initial increase in inflammatory M1 macrophages and is followed by a lesser increase in the anti-

inflammatory M2 macrophages [9,10]. Altogether, the upregulation in M2 macrophages by the T-cell deficient Achilles tendon injury model may provide not only a protective role but may also exhibit a pattern of healing that more closely resembles regeneration compared to its genetic controls.

Conclusion

This study is not without limitations. First, nude mice are created by ablating *Foxn1* expression. Although we reported a significant change in healing by the T-lymphocyte deficient nude mouse, we did not look further into mechanisms beyond the presence of T-lymphocytes. Thus, the effects on healing could be due to the role of T-lymphocytes and/or the *Foxn1* deficiency, and this experimental design was unable to distinguish possible mechanisms described above. Second, we did not distinguish the different types of T-lymphocytes and the role each plays in tendon healing. We appreciate that different phenotypes of T-lymphocytes (e.g. T-helper (Th), Natural Killer T cells (NKT), regulatory T cells (T_{reg}), etc), all have significant and differing roles in healing and regeneration. Based on the results of this study, a more thorough study to examine the contributions of the different phenotypes appears warranted. Third, we did not distinguish the sub-phenotypes of the M2 macrophages. The sub-phenotypes exert differing roles in the healing cascade, so the composition of sub-phenotypes should be explored in the future. Lastly, we did not perform additional protein analysis methods to support our IHC findings. Additional studies should examine the mechanisms of immune regulation on musculoskeletal healing.

In conclusion, musculoskeletal healing is a scar forming process that results in tissue that is mechanically weaker and more prone to re-rupture. Understanding the biological mechanisms to guide therapeutic improvement to the healing process would be a great benefit. As this study suggests, a reduction of T-lymphocytes and consequent increase in M2 macrophages improves musculoskeletal healing, possibly by serving a protective or accelerating role. More detailed analyses are necessary to identify the specific mechanisms involved to enhance tissue repair. Overall, the clinical implication of modulating the immune cells to stimulate healing are profound. It may be possible to manipulate certain subsets of T-lymphocytes and/or macrophages at specific healing stages to significantly enhance musculoskeletal healing. Such an approach merits further investigation.

Declaration of Interest

No competing financial interests exist.

Acknowledgement

The authors would like to acknowledge Allison P. Goeke, Lorenzo Manalo, Yunji Joo, Kaitlyn Gabardi, and Linzie A. Wildenauer for their technical support. Financial support was provided by the Orthopaedic Research and Education Foundation (OREF) under grant numbers MSN180250 and MSN197479. The content is solely the responsibility of the authors and does not necessarily represent the official views of the OREF.

References

1. Levenson SM, Geever EF, Crowley LV, Oates JF, Berard CW, et al. (1965) The Healing of Rat Skin Wounds. *Ann Surg* 161:293-308.

2. Lin TW, Cardenas L, Soslowsky LJ (2004) Biomechanics of tendon injury and repair. *J Biomech* 37: 865-877.
3. Patruno M, Martinello T (2014) Treatments of the injured tendon in Veterinary Medicine: from scaffolds to adult stem cells. *Histol Histopathol* 29: 417-422.
4. Yang G, Rothrauff BB, Tuan RS (2013) Tendon and ligament regeneration and repair: clinical relevance and developmental paradigm. *Birth Defects Res C Embryo Today* 99: 203-222.
5. Aktas E, Chamberlain CS, Saether EE, Duenwald-Kuehl SE, Kondratko-Mittnacht J, et al. (2017) Immune modulation with primed mesenchymal stem cells delivered via biodegradable scaffold to repair an Achilles tendon segmental defect. *J Orthop Res* 35: 269-280.
6. Chamberlain CS, Breiner AB, Kink JA, Choi U, Baer G, et al. (2019) Exosome-educated macrophages promote early Achilles tendon healing. *Stem Cells* 37: 652-662.
7. Clements AE, Chamberlain CS, Leiferman EM, Murphy WL, 0020Vanderby R (2017) Impacts of Interleukin-17 Neutralization on the Inflammatory Response in a Healing Ligament. *J Cytokine Biol* 2: 113.
8. Chamberlain CS, Leiferman EM, Frisch KE, Wang SJ, Yang XP, et al. (2011) The influence of macrophage depletion on ligament healing. *Connect Tissue Res* 52: 203-211.
9. Kawamura S, Ying L, Kim HJ, Dynybil C, Rodeo SA (2005) Macrophages accumulate in the early phase of tendon-bone healing. *J Orthop Res* 23: 1425-1432.
10. Chamberlain CS, Crowley E, Vanderby R (2009) The spatio-temporal dynamics of ligament healing. *Wound Repair and Regeneration* 17: 206-215.
11. Chamberlain CS, Duenwald-Kuehl SE, Okotie G, Brounts SH, Baer GS, et al. (2013) Temporal Healing in Rat Achilles Tendon: Ultrasound Correlations. *Ann Biomed Eng* 41: 477-487.
12. Muir P, Kelly JL, Marvel SJ, Heinrich DA, Schaefer SL, et al. (2011) Lymphocyte populations in joint tissues from dogs with inflammatory stiffler arthritis and associated degenerative cranial cruciate ligament rupture. *Vet Surg* 40: 753-761.
13. Faldyna M, Leva L, Knotigova P, Toman M (2001) Lymphocyte subsets in peripheral blood of dogs--a flow cytometric study. *Vet Immunol Immunopathol* 82: 23-37.
14. Wojciak B, Crossan JF (1993) The accumulation of inflammatory cells in synovial sheath and epitenon during adhesion formation in healing rat flexor tendons. *Clin Exp Immunol* 93: 108-114.
15. Wojciak B, Crossan JF (1994) The effects of T cells and their products on in vitro healing of epitenon cell microwounds. *Immunology* 83: 93-98.
16. Chamberlain CS, Leiferman EM, Frisch KE, Wang SJ, Yang XP, et al. (2011) The influence of interleukin-4 on ligament healing. *Wound Repair and Regeneration* 19: 426-435.
17. Nehls M, Pfeifer D, Schorpp M, Hedrich H, Boehm T (1994) New member of the winged-helix protein family disrupted in mouse and rat nude mutations. *Nature* 372: 103-107.
18. Barbul A, Shawe T, Rotter SM, Efron JE, Wasserkrug HL, et al. (1989) Wound healing in nude mice: a study on the regulatory role of lymphocytes in fibroplasia. *Surgery* 105: 764-769.
19. Gawronska-Kozak B (2011) Scarless skin wound healing in FOXP1 deficient (nude) mice is associated with distinctive matrix metalloproteinase expression. *Matrix Biol* 30: 290-300.
20. Velardo MJ, Burger C, Williams PR, Baker HV, Lopez MC, et al. (2004) Patterns of gene expression reveal a temporally orchestrated wound healing response in the injured spinal cord. *J Neurosci* 24: 8562-8576.
21. Chamberlain CS, Lee JS, Leiferman EM, Maassen NX, Baer GS, et al. (2015) Effects of BMP-12-Releasing Sutures on Achilles Tendon Healing. *Tissue Eng Part A* 21: 916-927.
22. Frisch KE, Marcu D, Baer GS, Thelen DG, Vanderby R (2014) The influence of partial and full thickness tears on infraspinatus tendon strain patterns. *J Biomech* Eng 136: 051004.
23. Frisch KE, Duenwald-Kuehl SE, Kobayashi H, Chamberlain CS, Lakes RS, et al. (2012) Quantification of collagen organization using fractal dimensions and Fourier transforms. *Acta Histochem* 114: 140-144.
24. Moisy F Boxcount (2008) Fractal dimension using the 'box-counting' method for 1D, 2D, and 3D sets.
25. Howell K, Chien C, Bell R, Laudier D, Tufa SF, et al. (2017) Novel Model of Tendon Regeneration Reveals Distinct Cell Mechanisms Underlying Regenerative and Fibrotic Tendon Healing. *Sci Rep* 7: 45238.
26. Lalley AL, Dymant NA, Kazemi N, Kenter K, Gooch C, et al. (2015) Improved biomechanical and biological outcomes in the MRL/MpJ murine strain following a full-length patellar tendon injury. *J Orthop Res* 33: 1693-1703.
27. Beredjikian PK, Favata M, Cartmell JS, Flanagan CL, Crombleholme TM, et al. (2003) Regenerative versus reparative healing in tendon: a study of biomechanical and histological properties in fetal sheep. *Ann Biomed Eng* 31: 1143-1152.
28. Clark LD, Clark RK, Heber-Katz E (1998) A new murine model for mammalian wound repair and regeneration. *Clin Immunol Immunopathol* 88: 35-45.
29. Ueno M, Lyons BL, Burzenski LM, Gott B, Shaffer DJ, et al. (2005) Accelerated wound healing of alkali-burned corneas in MRL mice is associated with a reduced inflammatory signature. *Invest Ophthalmol Vis Sci* 46: 4097-4106.
30. Leferovich JM, Bedelbaeva K, Samulewicz S, Zhang XM, Zwas D, et al. (2001) Heart regeneration in adult MRL mice. *Proc Natl Acad Sci USA* 98: 9830-9835.
31. Donnelly DJ, Popovich PG (2008) Inflammation and its role in neuroprotection, axonal regeneration and functional recovery after spinal cord injury. *Exp Neurol* 209: 378-388.
32. Thuret S, Thallmair M, Horky LL, Gage FH (2012) Enhanced functional recovery in MRL/MpJ mice after spinal cord dorsal hemisection. *PLoS One* 7: e30904.
33. Chircop MP, Yu Y, Berney CR, Yang JL, Crowe PJ, et al. (2002) Wound healing and growth factor expression in T lymphocyte deficiency. *ANZ J Surg* 72: 491-495.
34. Barbul A, Breslin RJ, Woodyard JP, Wasserkrug HL, Efron G (1989) The effect of in vivo T helper and T suppressor lymphocyte depletion on wound healing. *Ann Surg* 209: 479-483.
35. Peterson JM, Barbul A, Breslin RJ, Wasserkrug HL, Efron G (1987) Significance of T-lymphocytes in wound healing. *Surgery* 102: 300-305.
36. Fishel RS, Barbul A, Beschoner WE, Wasserkrug HL, Efron G (1987) Lymphocyte participation in wound healing. Morphologic assessment using monoclonal antibodies. *Ann Surg* 206: 25-29.
37. Lin KK, Chudova D, Hatfield GW, Smyth P, Andersen B (2004) Identification of hair cycle-associated genes from time-course gene expression profile data by using replicate variance. *Proc Natl Acad Sci USA* 101: 15955-15960.
38. Baxter RM, Brissette JL (2002) Role of the nude gene in epithelial terminal differentiation. *J Invest Dermatol* 118: 303-309.
39. Kur-Piotrowska A, Kopcewicz M, Kozak LP, Sachadyn P, Grabowska A, et al. (2017) Neotenic phenomenon in gene expression in the skin of Foxn1-deficient (nude) mice-a projection for regenerative skin wound healing. *BMC Genomics* 18: 56.
40. Efron JE, Frankel HL, Lazarou SA, Wasserkrug HL, Barbul A (1990) Wound healing and T-lymphocytes. *J Surg Res* 48: 460-463.
41. Park JE, Barbul A (2004) Understanding the role of immune regulation in wound healing. *Am J Surg* 187: 11S-16S.
42. Schaffer M, Barbul A (1998) Lymphocyte function in wound healing and following injury. *Br J Surg* 85: 444-460.
43. Choi Y, Simon-Stoos K, Puck JM (2002) Hypo-active variant of IL-2 and associated decreased T cell activation contribute to impaired apoptosis in autoimmune prone MRL mice. *Eur J Immunol* 32: 677-685.
44. Sharp AK, Colston MJ (1984) Elevated macrophage activity in nude mice. *Exp Cell Biol* 52:44-47.

-
45. Hato T, Winfree S, Kalakeche R, Dube S, Kumar R, et al. (2015) The macrophage mediates the renoprotective effects of endotoxin preconditioning. *J Am Soc Nephrol* 26: 1347-1362.
46. Luo XQ, Li A, Yang X, Xiao X, Hu R, et al. (2018) Paeoniflorin exerts neuroprotective effects by modulating the M1/M2 subset polarization of microglia/macrophages in the hippocampal CA1 region of vascular dementia rats via cannabinoid receptor 2. *Chin Med* 13: 14.
47. Godwin JW, Pinto AR, Rosenthal NA (2013) Macrophages are required for adult salamander limb regeneration. *Proc Natl Acad Sci USA* 110: 9415-9420.